EELS Quantification of Ca and Y Segregation Behaviors in Magnesium Aluminate Spinel

Alexander Campos-Quiros, Animesh Kundu, Masashi Watanabe

Microscopy and Microanalysis, **30** (Suppl 1), 2024, 1392–1393
https://doi.org/10.1093/mam/ozae044.684

Microscopy AND Microanalysis

Meeting-report

EELS Quantification of Ca and Y Segregation Behaviors in Magnesium Aluminate Spinel

Alexander Campos-Quiros[1,*], Animesh Kundu[1], and Masashi Watanabe[1]

[1]*Department of Materials Science and Engineering, Lehigh University, Bethlehem, PA, USA*

*Corresponding author: ajc420@lehigh.edu

Doping in ceramic materials, even at parts per million (ppm) levels, and subsequent grain-boundary (GB) segregation can have tremendous effects on several properties such as mechanical, electronic, magnetic, and optical properties as well as sintering and annealing behaviors with grain growth [1]. However, due to the low concentration typically used for doping to avoid secondary phase formation, the detailed characterization of the segregation behaviors can be challenging. Some aspects of interest that can help to close the knowledge gap between the segregation behaviors and the observed enhanced properties mentioned above are the segregation levels, spatial distribution of segregants and host atoms at GBs, and the exact position of individual doping atoms at the GBs. In the case of complex oxides, such as magnesium aluminate spinel (MAS, $MgAl_2O_4$), where two different types of cations sublattices are present (tetrahedral Mg^{2+} and octahedral Al^{3+} sites), determination of the dopant site occupancies within these two sublattices is highly important to elucidate the effect of doping on the GB properties. For example, previous studies by Cao et al. [2] have demonstrated that the GB fracture toughness can be increased up to 30% of that in the undoped condition by doping Yb^{3+} cations. However, when a different dopant element Eu^{2+} is used, the change in the GB fracture toughness is negligible [3]. Therefore, in this study, MAS was doped with two inexpensive and earth-abundant cations Y^{3+} and Ca^{2+} to study the segregation behaviors by quantitative electron-energy loss spectrometry (EELS), and to correlate with the mechanical behaviors.

Polycrystalline Ca- and Y-doped MAS samples were synthesized by hot-pressing and subsequently annealed at 1400 °C for 48 h in air (Ca-doped MAS) and N_2/H_2 (Y-doped MAS) atmospheres. Then, electron-transparent thin specimens were extracted from those doped samples using a focused-ion beam (FIB) instrument (Thermo/Fisher Scientific Electron transparent thin specimens Scios) operated at 30 kV. Damaged layers on the surface of FIB-prepared thin specimens were removed by gentle Ar-ion milling at 900 eV using a Fischione 1040 nanomill instrument. EELS analysis was performed using a CEOS energy filtering and imaging device (CEFID) equipped with a hybrid-pixel electron detector Dectris ELA in an aberration-corrected scanning transmission electron microscope (STEM) JEOL JEM-ARM200CF operated at 200 kV. Spectrum-imaging (SI) datasets were acquired in the vicinity of the GBs with an energy dispersion of 1.77 eV/channel over a range of 1820 eV for Ca-doped MAS and 3.48 eV/channel over a range of 3580 eV for Y-doped MAS including both the highly intense zero-loss peak (ZLP) and all low-intensity edges in a single spectrum. A convergence semi-angle α of 34 mrad was used for both specimens and collection semi-angles β of 60 and 35 mrad were used for Ca- and Y-doped MAS respectively. Furthermore, the acquisition of the SI datasets was performed using CEOS Panta Rhei software. Principal component analysis (PCA) in Digital Micrograph software was performed to remove random noise and quantitative analysis was performed using the Hartree-Slater ionization cross-section model.

Figures 1 show the quantified EELS maps in the vicinity of a GB for Ca- (top row) and Y-doped MAS (bottom row). The relative thickness for both specimens in the analyzed area was below 0.7 t/λ, and therefore plural scattering deconvolution was ignored in the analysis. A HAADF-STEM image in Figure 1 (a) shows no enhanced intensity indicating Ca segregation around the GB, mainly due to relatively insignificant atomic-number differences between Ca and host cations Mg and Al. Conversely, Figure 1 (f) shows enhanced intensities at the GB position, indicating the presence of Y segregation at the GB. It should be noted that some small particles corresponding to Pt which were redeposited from the protective layer during the FIB-specimen fabrication were found throughout both Ca- and Y-doped MAS specimens, but these particles did not affect the quantitative analysis in any significant form. The quantified EELS results showed that both specimens presented clear segregation of the corresponding doping elements at the GB, either Ca (Figure 1b) or Y (Figure 1g). In the case of Ca-doped MAS, Mg depletion was found at the GB together with Al excess, which suggests that Ca dopant atoms simply occupy Mg tetrahedral sites at the GB.

Similar to the Ca-doped condition, the Y-doped MAS sample presented Mg depletion at the GB but also Al depletion, whereas the Y segregation was found at the GB. This suggests that Y^{3+} cations preferentially occupy octahedral Al^{3+} sites at the GB, which was proven by direct observation through atomic-resolution HAADF-STEM imaging of several GBs; the positions of individual Y atoms match those of Al sites. For clearer visualization of the spatial distribution of the different elements in the GBs vicinities, concentration profiles were extracted from the dotted boxes in Figure 1 and shown in Figure 2. The current results evidence the potential of EELS quantitative analysis to characterize segregation behaviors of doping elements in MAS and selectively doping targeting specific cation sublattices for enhanced properties [4].

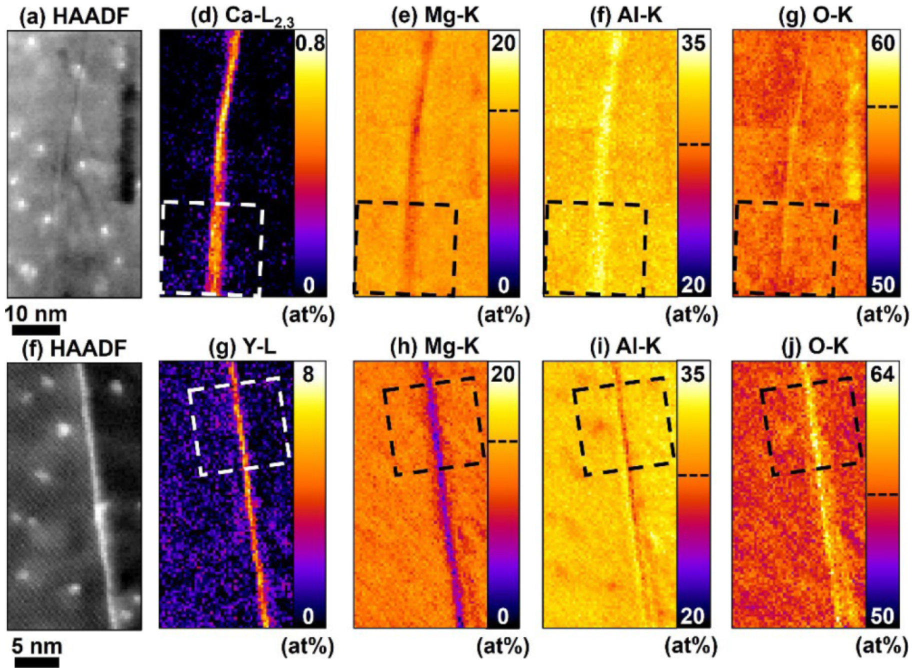

Figure 1. EELS-SI datasets obtained simultaneously acquired with HAADF-STEM images in the vicinity of GBs in Ca-doped MAS (top row) and Y-doped MAS (bottom row). Quantitative analysis in relative composition for (b) Ca-$L_{2,3}$, (c) Mg-K, (d) Al-K and (e) O-K edges for Ca-doped MAS and (g) Y-L, (h) Mg-K, (i) Al-K and (j) O-K edges for Y-doped MAS.

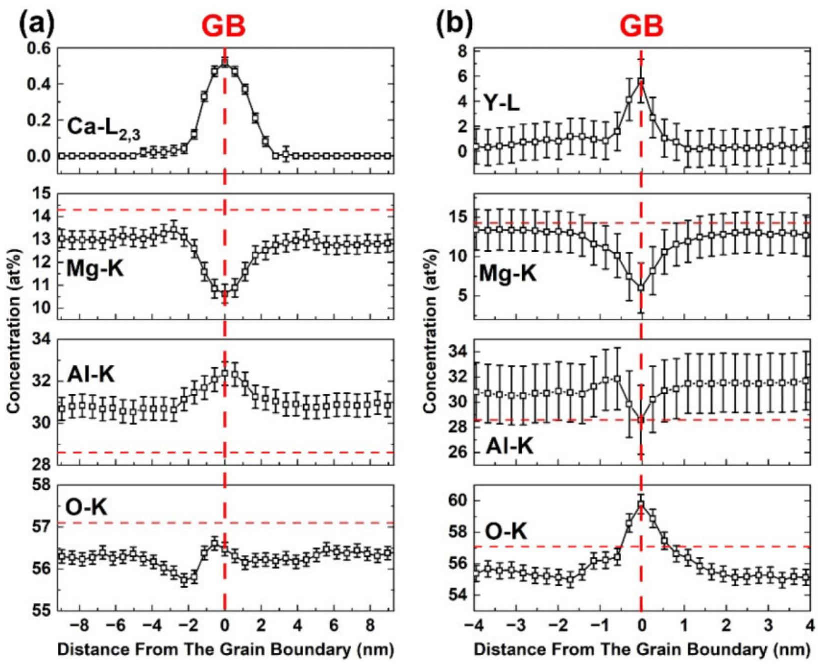

Figure 2. Composition profiles from the dotted boxes shown in Figure 1 (b-e) and (g-j) for Ca- and Y-doped MAS respectively. Error bars correspond to 99% confidence level (±3σ).

References

1. H. Vahidi, *et al.*, *Crystals* **11** (2021) 878. https://doi.org/10.3390/cryst11080878
2. W. Cao *et al.*, *Scr. Mater.* **69** (2013) 81–84. https://doi.org/10.1016/j.scriptamat.2013.03.002.
3. F. Cui, et al., *Acta Mater*, **148** (2018) 320–329. https://doi.org/10.1016/j.actamat.2018.01.039
4. The authors wish to acknowledge financial support from the NSF through grants DMR-2018683 and CMMI-2016279.